

Electrospun Scaffolds of a Polyhydroxyalkanoate Consisting of ω -Hydroxypentadecanoate Repeat Units: Fabrication and *In Vitro* Biocompatibility Studies

Maria Letizia Focarete^{a,*}, Chiara Gualandi^a, Mariastella Scandola^a, Marco Govoni^b, Emanuele Giordano^b, Laura Foroni^c, Sabrina Valente^c, Gianandrea Pasquinelli^d, Wei Gao^e and Richard A. Gross^e

^a University of Bologna, Department of Chemistry 'G. Ciamician' and National Consortium of Materials Science and Technology (INSTM, RU Bologna), via Selmi 2, 40126 Bologna, Italy

^b University of Bologna, Department of Biochemistry 'G. Moruzzi' and National Institute for Cardiovascular Research (INRC, RU Cesena), via Imerio 48, 40126 Bologna, Italy

^c University of Bologna, Anaesthesiological and Surgical Sciences, via Massarenti 9, 40138 Bologna, Italy

^d University of Bologna, Clinical Department of Radiological and Histocytomorphological Sciences, via Massarenti 9, 40138 Bologna, Italy

^e NSF-I/UCRC Center for Biocatalysis and Bioprocessing of Macromolecules, Polytechnic Institute of NYU, Department of Chemical and Biological Science, Six Metrotech Center, Brooklyn, NY-11201, USA

Received 29 April 2009; accepted 23 July 2009

Abstract

Electrospinning was used to fabricate fibrous scaffolds of lipase-catalyzed poly(ω -pentadecalactone) (PPDL). The slow resorbability of this biomaterial is expected to be valuable for tissue-engineering applications requiring long healing times. The effect of solvent systems and instrumental parameters on fiber morphology was investigated. PPDL electrospinning was optimized and defect-free fibers (diameter 410 ± 150 nm) were obtained by using a mixed three-solvent system. Scaffolds were characterized by scanning electron microscopy, thermogravimetric analysis (TGA), differential scanning calorimetry (DSC) and wide angle X-ray diffraction (WAXS). TGA showed no residual solvent in the scaffolds. DSC and WAXS results indicated that electrospun PPDL is semicrystalline. Biocompatibility of PPDL scaffolds was evaluated through indirect cytotoxicity tests using embryonic rat cardiac H9c2 cells. The ability of PPDL electrospun mats to support cell growth was verified by culturing H9c2 cells onto the scaffold. Cell adhesion, proliferation and morphology were evaluated. The results indicated that PPDL mats are not cytotoxic and they support proliferation of H9c2 cells. The cumulative results of this study suggest further exploration of PPDL fibrous mats as scaffolds for tissue-engineered constructs.

© Koninklijke Brill NV, Leiden, 2010

* To whom correspondence should be addressed. Tel.: (39-51) 209-9572; Fax: (39-51) 209-9456; e-mail: marialetizia.focarete@unibo.it

Keywords

Electrospinning, poly(ω -pentadecalactone), polyesters, biomaterials, tissue engineering, embryonic rat cardiac H9c2 cells, biocompatibility

1. Introduction

Synthetic aliphatic polyesters are widely used as temporary scaffold materials for tissue engineering applications where bioresorbability is a key feature [1, 2]. This class of polymers is completely hydrolysable in physiological conditions, with degradation times ranging from days to years, depending on polymer composition and molecular weight. In particular, poly(α -hydroxy esters) such as poly(lactic acid) (PLA), poly(glycolic acid) (PGA) and their co-polymers have been intensively investigated as biomaterials in therapeutic applications where a controlled biodegradation rate is required [1, 2]. Another widely used medical-grade polyester is poly(ϵ -caprolactone) (PCL) whose lower hydrophilicity leads to slower degradation kinetics than lactide/glycolide-based polymers. Commonly adopted strategies to design polymeric biomaterials with tailored properties and degradation rates are both co-polymerization of different hydroxy acid or lactone monomers and blending of bioresorbable polyesters with different hydrophilicity [3, 4].

A highly hydrophobic synthetic aliphatic polyester is poly(ω -pentadecalactone) (PPDL). This long-chain polymer, with 14 methylene units per ester group, combines the advantage of being hydrolyzable, owing to the presence of ester bonds in the polymer chain, with mechanical properties comparable to those of polyethylene (PE) [5]. Both PCL, which is already used as a biomaterial, and PPDL, are crystalline polyesters. However PPDL, that melts around 97°C [5], may be more suitable for a broad range of applications than PCL, that melts at a lower temperature (T_m around 60°C).

PPDL is synthesized from the macrocyclic lactone PDL through lipase-catalyzed ring-opening polymerization (ROP) [6]. This biocatalytic route circumvents use of heavy metal catalysts [7] that must otherwise be removed prior to biomaterial use. Furthermore, by conducting reactions at lower temperatures than when using chemical catalysis, less unwanted by-products are formed. These are key issues that must be considered in order for biomaterials to meet strict purity and biocompatibility requirements. In addition, advances in lipase-catalyzed ROP now allow synthesis of high molecular weight polymers and some lipases such as *Candida antarctica* lipase B (CALB) are sufficiently promiscuous that they allow incorporation of different monomers along chains so that co-polymers with defined composition and microstructure can be prepared. Indeed, PDL has been successfully co-polymerized with comonomers such as trimethylene carbonate [8], ϵ -caprolactone [9] and *p*-dioxanone [10], thus enabling material scientists to ‘tailor’ corresponding biomaterial physical properties and hydrolysis rate for targeted applications.

In the field of tissue engineering, PPDL homo-polymer is an interesting candidate that would provide slow-resorbability for applications where long healing

times are required. A very recent paper by van der Meulen *et al.* [11] demonstrated that a PPDL bulk sample, synthesized *via* enzymatic ROP, has no indirect cytotoxic effects on mammalian fibroblasts.

Tissue engineering scaffolds mimicking the nanoscale features of native extracellular matrix (ECM) are commonly obtained, in the form of nanofibrous structures, by means of three main approaches: self-assembly, phase separation and electrospinning [12–14]. These techniques are based on a very different experimental approach and provide sub-micrometer fibers with different diameter ranges. Self-assembly generates fibers with diameter in the lowest end of the range of ECM fibers, phase separation provides fibers in the same dimensional range of ECM, and diameter of fibers obtained by means of electrospinning is typically in the upper range of those of ECM. Due to its versatility electrospinning has been recognized as a powerful scaffold fabrication technology yielding non-woven fibrous meshes. It is widely used to obtain continuous polymeric fibers from a wide range of polymer solutions and melts [15–20]. Moreover, electrospinning provides control not only of fiber morphology but also of fiber deposition pattern [21]. This aspect is very important since the micro/nano-architecture of the scaffold (i.e., fiber size and orientation) is expected to influence cell behavior [22, 23].

This work describes the main steps of electrospinning process optimization that lead to fabrication of PPDL mats made of defect-free sub-micrometric fibers. Moreover, in view of potential biomedical applications of electrospun PPDL scaffolds, their biocompatibility towards mammalian cells is evaluated using the H9c2 cell line as an *in vitro* benchmark to test indirect cytotoxicity as well as cell adhesion, proliferation and morphology.

2. Materials and Methods

2.1. Scaffold Fabrication and Characterization

Poly(ω -pentadecalactone) (PPDL) ($M_n = 64$ kg/mol, polydispersity index (PDI) = 2) was synthesized as described previously [6]. Chloroform (CLF), dichloromethane (DCM) and 1,1,3,3,3-Hexafluoro-2-propanol (HFIP) were used as solvents. All solvents were purchased from Sigma-Aldrich and used without further purification.

The electrospinning apparatus made in house was composed of a high voltage power supply (Spellman SL 50 P 10/CE/230), a syringe pump (KDSscientific 200 series), a glass syringe, a stainless-steel blunt-ended needle (inner diameter 0.51 mm) connected with the power supply electrode and a grounded aluminum plate-type collector (7×7 cm). The polymer solution was dispensed, through a Teflon tube, to the needle vertically placed on the collecting plate.

A series of PPDL polymer solutions (polymer concentration 5–10% (w/v)) were prepared using different solvent mixtures, as described in the Results and Discussion section. The electrospinning process was performed at room temperature (RT)

and relative humidity in the range 40–50%. The obtained electrospun scaffolds were kept under vacuum in a desiccator overnight in order to eliminate residual solvents.

Scanning electron microscopy (SEM) observations were carried out using a Philips 515 microscope at an accelerating voltage of 15 kV, on samples sputter-coated with gold. Fiber diameter distribution (300 fibers analyzed for each sample) was estimated using the EDAX Genesis acquisition and image analysis software. Thermogravimetric analysis (TGA) measurements were performed with a TA Instruments TGA2950 Thermogravimetric Analyzer from RT to 600°C (heating rate 10°C/min, purge gas nitrogen). Differential scanning calorimetry (DSC) was carried out using a TA Instruments Q100 DSC equipped with the LNCS low-temperature accessory. DSC scans (20°C/min) were performed in the temperature range from –100°C to 150°C. Wide angle X-ray diffraction measurements (WAXS) were carried out at RT with a PANalytical X'Pert PRO diffractometer equipped with an XCelerator detector. Cu anode was used as X-ray source ($\lambda_1 = 0.15406$ nm, $\lambda_2 = 0.15443$ nm). The amorphous and crystalline contributions were calculated by fitting method using the WinFit program [24]. The degree of crystallinity (χ_c) was evaluated as the ratio of the crystalline peak areas to the total area under the scattering curve [25].

2.2. Biocompatibility Evaluation

2.2.1. Indirect Cytotoxicity Test

Indirect cytotoxicity evaluations of electrospun PDDL scaffolds were performed in accordance with the ISO10993-5 international standard for biological evaluation of medical devices. Culture medium and culture reagents were purchased from BioWhittaker. PDDL mats were sterilized in a laminar flow culture hood by immersion in 70% ethanol for 15 min, followed by repeated washes in phosphate-buffered saline (PBS) + 100 U/ml penicillin/streptomycin (pen/strep). To obtain the medium containing the PDDL extract (PDDL-extract medium), PDDL mats (5 mg polymer/1 ml medium) were kept in Dulbecco's modified Eagle's medium (DMEM) supplemented with 10% heat-inactivated fetal bovine serum (FBS), 2 mM L-glutamine and 100 U/ml pen/strep, at 37°C in a humidified atmosphere containing 5% CO₂ for 24 h. PDDL-extract medium was filtered through a 0.2 µm porosity nitrocellulose filter before administration to embryonic rat cardiac H9c2 cells, obtained from the European Collection of Cell Cultures (ECACC). Cells were seeded in a 96-well culture plate (500 cells/well) in standard DMEM to allow their attachment. After 48 h, the culture medium was discarded, the PDDL-extract medium was added to the wells and the cells were further incubated for 24 h. At the end of this incubation period cells were quantified by the sulforhodamine B (SRB) colorimetric assay for cytotoxicity screening [26]. Optical density ($\lambda = 540$ nm) of samples was read in a Wallac Victor multilabel multiplate reader (Perkin Elmer). Two separate experiments, six replicates each, were performed. The signal obtained from cells cultured in DMEM was used as the negative control. A cytotoxic response (positive control) was obtained by addition of 1 mM H₂O₂ for 120 min to cells (48 h after

cell seeding). Optical density mean values \pm standard error of the mean (SEM) for replicates were calculated and the unpaired *t*-test was used to evaluate statistical differences between mean values.

2.2.2. Cell Adhesion and Proliferation

Evaluation of both cell adhesion and cell proliferation was performed in accordance with ISO10993-5, the international standard for biological evaluation of medical devices. For this purpose, a plastic ring (Teflon, internal diameter 17 mm, external diameter 20 mm) was fixed to a PDDL mat using silicone rubber (RTV 108Q, GE Silicones), in order to obtain a cell leakage-proof well with the PDDL scaffold fixed at the bottom and also to prevent scaffold shrinkage during the sterilization procedure. Sterilization was performed in a laminar flow culture hood by immersion in 70% ethanol for 15 min, followed by washings in PBS + 200 U/ml pen/strep + 0.2% fungizone (Sigma Aldrich). In order to evaluate cell adhesion and proliferation on the electrospun scaffold, 2.5×10^4 H9c2 cells in 1 ml DMEM were seeded onto the PDDL mat, assembled with the Teflon ring as described above, and placed in standard culture multiplates. The number of viable cells was quantified every other day, up to 14 days, with the Alamar Blue fluorescence assay (Invitrogen) [27]. Alamar Blue fluorescence (Ex/Em = 540/590 nm) was read in a Wallac Victor multilabel multiplate reader (Perkin Elmer). Control signal was acquired from H9c2 cells cultured in standard polystyrene wells (Sarstedt). Four separate experiments ($n = 4$), three replicates each, were performed. Two-way analysis of variance (ANOVA) was performed to compare proliferation curves. Values were given as the mean values of fluorescence \pm SEM.

2.2.3. Morphology of Cultured Cells

Scanning electron microscopy was used to assess interactions of H9c2 cells with PDDL scaffolds after culture experiments. After 14 days in culture, PDDL mats were washed with 0.15 M phosphate buffer in order to remove culture medium and were then fixed in 2.5% buffered glutaraldehyde overnight at 4°C. After further rinses, the PDDL scaffold was carefully removed from the Teflon ring with a scalpel and post-fixed in 1% osmium tetroxide for 15 min at room temperature. The scaffolds were washed with distilled water, dehydrated by increasing ethanol concentration (70%, 96% and 100%; 15 min each step) and, finally, dried with hexamethyldisilazane (HMDS, Fluka). Dehydrated samples were placed in a 1:1 solution of absolute ethanol and HMDS and then transferred in pure HMDS for 30 min at room temperature. Scaffolds were mounted on aluminum stubs (Multilab Type stub pin 1/2") using double-sided adhesive tape, coated with a 10 nm thick layer of gold in a Balzers MED 010 sputtering device and subsequently they were observed using a Philips SEM 515 at 15 kV.

3. Results and Discussion

3.1. Scaffold Fabrication and Characterization

This paper reports the first optimization study aimed at electrospinning PPDL to fabricate sub-micrometric fibrous scaffolds for tissue-engineering applications. The electrospinning technique allows tailoring of fiber diameter and morphology by manipulating a combination of variables including: (i) solution properties (molecular weight and concentration of polymer; electrical properties, boiling point and surface tension of the solution); (ii) instrumental parameters (applied voltage, needle to collector distance, solution flow rate, needle diameter) and (iii) environmental parameters (temperature and relative humidity). None of these variables functions independently. In contrast, their influence is closely interconnected and overall control of fiber morphology requires systematic investigations.

The main solution properties that affect fiber morphology are polymer molecular weight and solution concentration [28, 29]. These two parameters determine the presence of polymeric chain entanglements that provide a viscoelastic polymer network required to prepare electrospun fibers [28, 30]. A progressive change from individual electrospayed beads to continuous electrospun fibers is usually observed as chain entanglement density increases in polymer solution.

In addition to the number of chain entanglements, the selected solvent system profoundly influences fiber morphology [31]. This is attributed to the fact that formation of the jet occurs when electrostatic charge repulsions overcome solution surface tension. Therefore, the approach to optimize PPDL electrospinning was as follows. First, different polymer concentrations and several solvent systems were investigated to address their influence on viscoelasticity, electrical properties and solution surface tension. Once a proper polymer solution was selected, instrumental parameters were then optimized to obtain defect-free sub-micrometer fibers.

Table 1 lists physical properties [32] of the most common solvents employed for electrospinning aliphatic polyesters and their ability to dissolve PPDL. Among the different solvents tested, chloroform (CLF) is the only pure organic solvent that dissolves PPDL at RT; therefore, solutions of PPDL were initially prepared in CLF. The minimum polymer concentration required to obtain the transition from electrospaying to electrospinning in CLF was 7% (w/v). This result is attributed to attaining a suitable degree of chain entanglements with increased solution viscosity. However, nanofibers obtained from this solution exhibited ‘bead’ defects. This type of defect is often eliminated by increasing polymer concentration that is accompanied by increased fiber diameter [28, 33, 34]. Upon increasing solution concentration from 7 to 10% (w/v) PPDL fibers with larger diameter were obtained, without elimination of the bead defects. Additional experiments by using 10% (w/v) PPDL solution and changing instrumental parameters (i.e., applied voltage, needle to collector distance and solution flow rate) did not significantly improve fiber morphology. Fong and Reneker [35] showed that formation of beads in electrospun fibers is predominantly determined by viscosity, charge density and

Table 1.Physical properties of selected solvents^a and their ability to solubilize PPDL

Solvent	PPDL solubility test	Boiling point (°C)	Dielectric constant (dyne/cm)	Surface tension (mN/m ²)
Chloroform (CLF)	Soluble	61	4.8	26.6
Dichloromethane (DCM)	Insoluble	40	8.9	27.2
1,1,3,3,3-Hexafluoro-2-propanol (HFIP)	Insoluble	58	16.7	16.1
Dimethylformamide	Insoluble	153	38.3	35.7
Acetone	Insoluble	56	21.0	22.7
Tetrahydrofuran	Insoluble	65	7.5	26.4
Methanol	Insoluble	65	33.0	22.1

Soluble, 1% (w/v) solution is optically clear at room temperature; insoluble, 1% (w/v) solution is not optically clear at room temperature.

^a From Ref. [32].

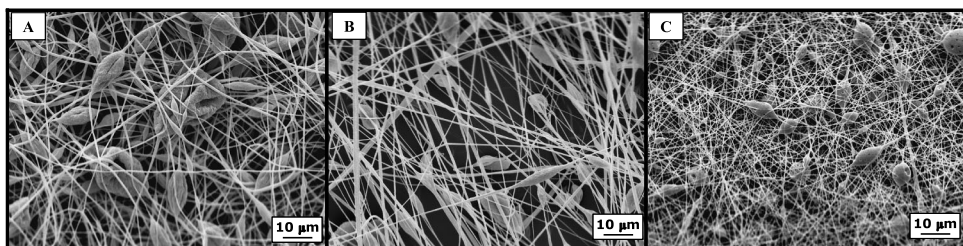


Figure 1. SEM micrographs of nanofibers obtained by electrospinning 5% (w/v) PPDL in different mixed solvents: (A) CLF/DCM = 50:50 (v/v), (B) CLF/DCM = 30:70 (v/v) and (C) CLF/HFIP = 80:20 (v/v). Applied voltage 15 kV, solution flow rate 0.2 ml/min and needle to collector distance 15 cm.

solution surface tension. Specifically, high viscosity, high charge density and low surface tension lead to production of defect-free fibers. In the case of the PPDL-CLF solutions, simply increasing solution viscosity did not prevent bead formation. Therefore, alternative mixed solvent systems were investigated in order to modify electrical properties and surface tension of electrospinning solutions.

First, CLF was mixed with DCM that has a higher dielectric constant than CLF (Table 1) so that the solution can carry a higher amount of charge [36]. This is based on the assumption that solvent properties do not change dramatically upon addition of PPDL [19]. As an example, Fig. 1A and 1B show SEM images of fibers obtained from 5% (w/v) PPDL solutions containing different amounts of DCM. By increasing DCM content in the mixed solvent from 50% to 70% by volume (Fig. 1A and 1B, respectively), fibers produced were thinner with more elongated beads. The minimum concentration (5% (w/v)) required to obtain PPDL fibers for CLF/DCM 50:50 (v/v) was lower than that for pure CLF (7% w/v). This result is

consistent with the hypothesis that the minimum concentration required for fiber formation depends not only on solution viscosity but also on the solution charge density and surface tension [31, 37]. CLF and DCM have similar surface tension (see Table 1), therefore, it is reasonable to suppose that the lower concentration required to electrospin PPDL in the presence of DCM is due to higher net charge density accumulated on the jet. Although the addition of high amounts of DCM to CLF improved fiber morphology, solidification at the needle tip occurred during the electrospinning process, due to DCM's low boiling point (see Table 1).

Based on the above, DCM was replaced with HFIP in the CLF solvent mixture. Relative to DCM, HFIP has a higher boiling point, higher dielectric constant and a lower surface tension (see Table 1). These characteristics are expected to improve fiber morphology by decreasing fiber diameter and preventing bead formation [35]. However, for 5% (w/v) PPDL solubilized in CLF, addition of >20% (v/v) HFIP resulted in PPDL precipitation. Figure 1C shows that PPDL fibers, electrospun from a 5% (w/v) solution consisting of 80:20 (v/v) CLF/HFIP using identical processing conditions as for fibers obtained from CLF/DCM mixtures (Fig. 1A and 1B), still contained beads. The main effect of substituting DCM with HFIP was decreasing PPDL fiber diameter. The presence of beads could not be reduced by further increasing HFIP content in the solvent mixture since increasing the concentration beyond 20% (v/v) resulted in PPDL precipitation.

In order to combine the properties of all solvents investigated, PPDL was dissolved in a ternary mixture of CLF, DCM and HFIP. After exploring several solvent compositions and PPDL concentrations, it was determined that preferred values were CLF/DCM/HFIP 50:40:10 (v/v) and 7% (w/v), respectively. The effect of instrumental parameters (applied voltage and solution flow rate) on fiber morphology was then investigated with the aim of obtaining sub-micrometric defect-free PPDL fibers. Figure 2 illustrates the effect of applied voltage on PPDL fiber morphology. Micrographs in Fig. 2 show that application of 16 kV (Fig. 2B) enabled production of uniform defect-free fibers, whereas when either lower (Fig. 2A) or higher voltages (Fig. 2C) were used, defects were still present and non-homogeneous fibers were obtained in agreement with previous findings [37]. Hence, an applied voltage of 16 kV was selected as the working voltage for determining effects of solution flow rate on fiber morphology. As shown in Fig. 3, since lower flow rate provides a smaller amount of solution to be stretched, decreasing the flow rate led to thinner PPDL fibers, as earlier described by Zhong *et al.* [34]. By using flow rates of 0.2, 0.1 and 0.05 ml/min, fibers were obtained with average diameters of 610 ± 210 nm, 530 ± 190 nm and 410 ± 150 nm, respectively.

On the basis of the above investigations, PPDL mats for biocompatibility evaluation were prepared by electrospinning a PPDL solution (7% (w/v)) in CLF/DCM/HFIP (50:40:10 (v/v)), using the following process conditions: applied voltage 16 kV, solution flow rate 0.05 ml/min and needle to collector distance 15 cm. Thermal and structural properties of PPDL electrospun mats were evaluated by thermogravimetric analysis (TGA), differential scanning calorimetry (DCS) and

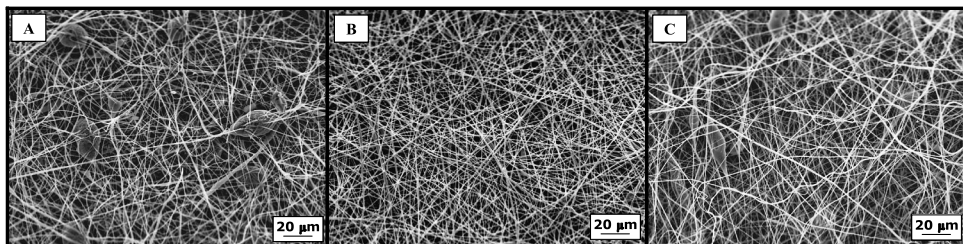


Figure 2. SEM micrographs of PPDL nanofibers electrospun from 7% (w/v) PPDL solution in CLF/DCM/HFIP (50:40:10 (v/v)) at different applied voltages: (A) 14 kV, (B) 16 kV and (C) 18 kV. Flow rate 0.1 ml/min, needle to collector distance 15 cm.

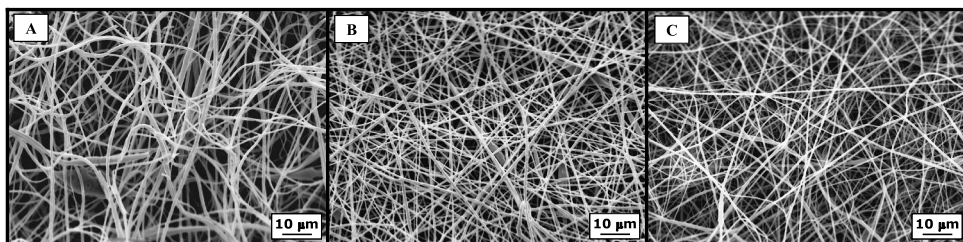


Figure 3. SEM micrographs of PPDL nanofibers electrospun from 7% (w/v) PPDL solution in CLF/DCM/HFIP (50:40:10 (v/v)) at different flow rates. (A) 0.2 ml/min, (B) 0.1 ml/min and (C) 0.05 ml/min. Applied voltage 16 kV, needle to collector distance 15 cm.

wide angle X-ray scattering (WAXS). TGA did not reveal the presence of residual solvent in mats. DSC analysis showed that PPDL in fiber mats had a peak T_m of 92°C and melting enthalpy (ΔH_m) of 125 J/g. In contrast, a non-electrospun bulk PPDL sample had $T_m = 98^\circ\text{C}$ and $\Delta H_m = 156$ J/g. The WAXS diffractograms (not shown) revealed that electrospun PPDL crystallizes in the same crystal lattice as starting PPDL but it develops a lower crystallinity degree ($\chi_c = 54\%$) than bulk PPDL ($\chi_c = 74\%$). The latter observation is consistent with DSC evidence that the melting enthalpy of electrospun PPDL was lower than that of the bulk polymer. Crystallization developed during electrospinning occurs concurrently with solvent evaporation and, therefore, changes in solvent content are expected to strongly influence crystallization kinetics. Several literature reports give examples of large decreases in the crystal fraction or even total inhibition of crystallization when electrospinning crystallizable polymers [34, 38, 39]. For PPDL, DSC and WAXS results show that the polyester maintains a remarkable ability to crystallize upon fiber solidification during the electrospinning process.

3.2. Biocompatibility Evaluation

In view of potential applications of PPDL scaffolds for *in vitro* cardiac tissue engineering, investigations were performed to evaluate cytotoxicity, cell adhesion and proliferation on PPDL fibrous substrates by using H9c2 myoblast cells derived from embryonic rat heart [40]. The sulforhodamine B (SRB) colorimetric assay [26] was

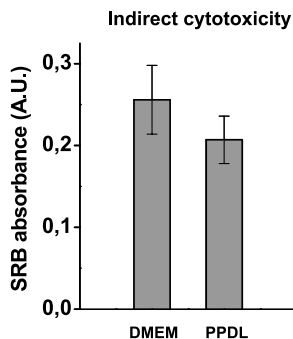


Figure 4. Evaluation of the indirect cytotoxicity of electrospun PPDL scaffolds. Sulforhodamine B (SRB) colorimetric assay of H9c2 cells cultured for 24 h in different media. DMEM, standard medium (negative control); PPDL, polymer extraction medium. Values are given as mean \pm SEM of the absorbance (a.u.) of 6 replicates of a representative experiment for each condition. PPDL was not statistically different from DMEM.

used to assess potential cytotoxicity of electrospun PPDL on H9c2 cells. Figure 4 shows that SRB absorption spectroscopy output was comparable for samples grown for 24 h in PPDL-extraction medium (0.21 ± 0.029 a.u.) or in standard DMEM medium (0.26 ± 0.042 a.u.). When exposed to 1 mM H_2O_2 for 120 min, as a positive cytotoxicity control, all the cells were killed (not shown). This result indicates the absence of potentially cytotoxic products released from PPDL, in agreement with the conclusion of recent indirect cytotoxicity tests [11] run on mouse fibroblast 3T3 cells treated with an extract from a PPDL bulk sample. This work demonstrates that PPDL non-cytotoxicity is maintained after scaffold fabrication *via* electrospinning, a procedure involving the use of solvents.

In order to investigate the suitability of PPDL electrospun mats to act as three-dimensional scaffolds for H9c2 cells, cell adhesion and proliferation were evaluated every other day for up to 14 days using the Alamar Blue (AB) fluorescence assay. The oxidized form of AB is taken into cells and reduced by their mitochondrial enzyme activity. This redox reaction is visually determined by a shift in color of the culture medium from non-fluorescent blue to fluorescent pink. Quantification was performed by fluorescence measurements on aliquots withdrawn from media. The same cell culture was monitored over time (14 days), thus overcoming drawbacks inherent to other sample-destructive proliferation assays, such as the MTT test [27]. Results reported in Fig. 5 show that, after 24 h from cell seeding, electrospun PPDL mats host about 50% of the number of H9c2 cells that adhere to the control polystyrene surface (Fig. 5, day 1). The number of cells growing onto PPDL increases linearly for up to day 14 (end of experiments), although a significant difference with respect to the number of the cells proliferating onto the standard culture plasticware is maintained at any given time point (ANOVA, $P < 0.0001$). These results show that PPDL fibrous substrates are not cytotoxic towards H9c2 cells and support cell proliferation. Indeed, when let to grow up to 4 weeks, H9c2

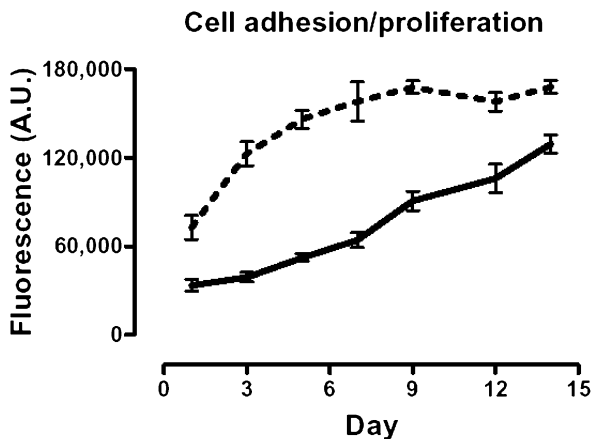


Figure 5. Evaluation of cell adhesion and proliferation on the electrospun PPDL scaffolds (continuous line) compared with polystyrene control (dotted line) by Alamar Blue fluorescence assay. Values are given as means \pm SEM of fluorescence arbitrary units of 4 separate experiments in triplicate. Control $P < 0.0001$ vs. PPDL.

cells reached the same maximum value obtained on the polystyrene support (data not shown). It is pointed out that over the 4 weeks experiment with H9c2 cells scaffolds maintained their integrity and no evidence of scaffold degradation was obtained by morphological and thermal investigations (results not shown), as expected given the chemical structure of this polyester with a low COO/CH₂ ratio.

The morphology of H9c2 cells grown onto electrospun PPDL mats was observed by scanning electron microscopy. Figure 6A and 6C shows that, after 14 days of culture, H9c2 cells propagate and spread over the PPDL mat surface while retaining their native, mesenchymal spindle-shaped, sheet-like morphology. Furthermore, at 14 days, the scaffold surface is almost entirely covered by cells. In the experiment where cells were allowed to grow over PPDL for up to 4 weeks, the PPDL surface appears completely covered with a cell monolayer that prevents visualization of underlying fibers (Fig. 6B and 6D). Scanning electron microscopic observation of cell morphology together with results provided by cytotoxicity test and AB assay confirm that PPDL in the form of electrospun fiber mats is biocompatible and able to promote H9c2 adhesion and proliferation.

4. Conclusions

This paper describes for the first time fabrication of sub-micrometric fibers of poly(ω -pentadecalactone) (PPDL) and shows that the obtained scaffolds are biocompatible. Biosynthesized PPDL is an interesting bioresorbable polyester that may find applications as tissue engineering scaffolds when long degradation times are required. The PPDL electrospinning process was successfully optimized and defect-free fibers were obtained using a mixed three-solvent system. Indirect cytotoxicity evaluation of PPDL fibrous mats, using H9c2 myoblast cells from em-

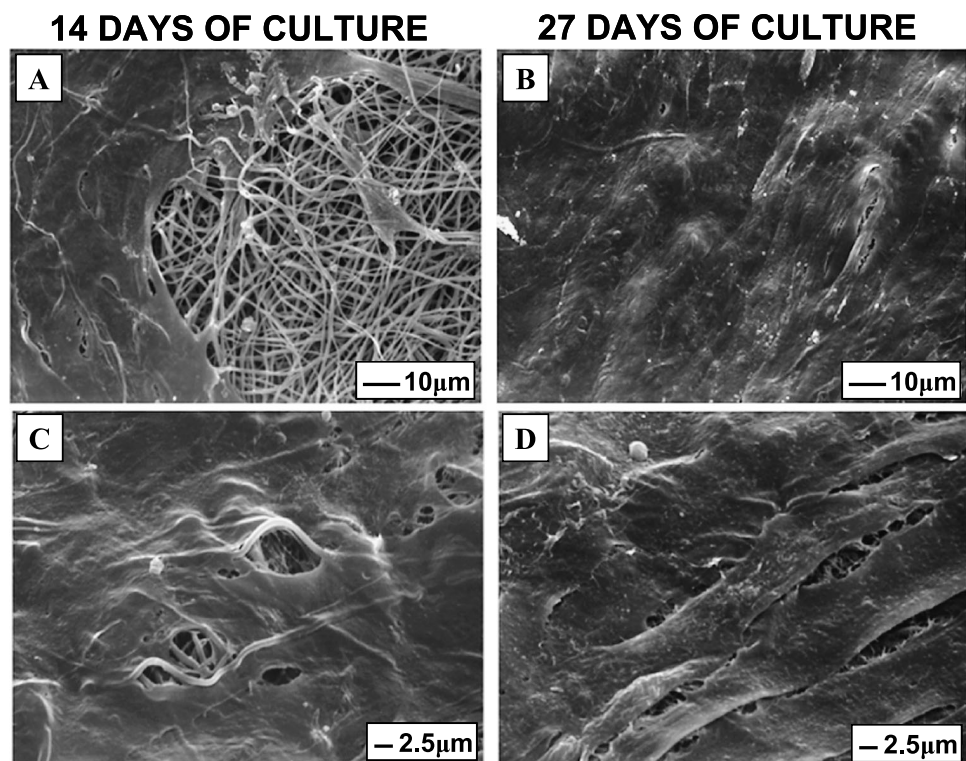


Figure 6. Scanning electron microscopy micrographs showing the interaction between H9c2 cells and PPDL electrospun scaffold after 14 days (A and C, two different magnifications) and 27 days of culture (B and D, two different magnifications).

bryonic rat heart, demonstrated that the scaffolds are non-toxic towards cells. The ability of electrospun PPDL scaffolds to support cell adhesion and to promote cell proliferation was assessed. H9c2 cells retain their native, mesenchymal spindle shaped, sheet-like morphology and cover the scaffold surface with a confluent cell monolayer. These results suggest that PPDL fibrous mats from electrospinning are promising slow-degrading biomaterial supports for tissue-engineering applications.

Acknowledgements

This work was partially supported by Strategic Project SCFELMED (University of Bologna), Italian Ministry of Foreign Affairs (Directorate General for Cultural Promotion and Cooperation — Significant Bilateral Project Italia-USA), Fondazione Cassa di Risparmio in Bologna (CARISBO 2007.0058), Regione Emilia Romagna (Programma di Ricerca Regione — Università 2007–2009, Area 1b ‘Medicina rigenerativa’). M. G. is the recipient of a fellowship awarded by National Institute for Cardiovascular Research (INRC) (funding from the Compagnia di San

Paolo, Torino). R. G. and W. G. thank the National Science Foundation Industry/University Cooperative Research Center (NSF-I/UCRC) for Biocatalysis and Bio-processing of Macromolecules at Polytechnic Institute of NYU for their financial support.

References

1. L. G. Griffith, *Acta Mater.* **48**, 263 (2000).
2. J. M. Pachence, M. P. Bohrer and J. Kohn, in: *Principles of Tissue Engineering*, R. Lanza, R. Langer and J. Vacanti (Eds), p. 322. Elsevier Science, Amsterdam (2007).
3. M. Hakkarainen, *Adv. Polym. Sci.* **157**, 113 (2002).
4. J. C. Middleton and A. J. Tipton, *Biomaterials* **21**, 2335 (2000).
5. M. L. Focarete, M. Scandola, A. Kumar and R. A. Gross, *J. Polym. Sci. Part B: Polym. Phys.* **39**, 1721 (2001).
6. K. S. Brisht, L. A. Henderson, R. A. Gross, D. L. Kaplan and G. Swift, *Macromolecules* **30**, 2705 (1997).
7. R. Nomura, A. Ueno and T. Endo, *Macromolecules* **27**, 620 (1994).
8. M. L. Focarete, M. Gazzano, M. Scandola and R. A. Gross, *Macromolecules* **35**, 8066 (2002).
9. G. Ceccorulli, M. Scandola, A. Kumar, B. Kalra and R. A. Gross, *Biomacromolecules* **6**, 902 (2005).
10. Z. Jiang, H. Azim, R. A. Gross, M. L. Focarete and M. Scandola, *Biomacromolecules* **8**, 2262 (2007).
11. I. Van der Meulen, M. de Geus, H. Antheunis, R. Deumens, E. A. J. Joosten, C. E. Koning and A. Heise, *Biomacromolecules* **9**, 3404 (2008).
12. L. A. Smith and P. X. Ma, *Colloids Surfaces B: Biointerfaces* **39**, 125 (2004).
13. H. Hosseinkhani, M. Hosseinkhani and H. Kobayashi, *Biomed. Mater.* **1**, 8 (2006).
14. H. Hosseinkhani, M. Hosseinkhani, A. Khademhosseini, H. Kobayashi and Y. Tabata, *Biomaterials* **27**, 5836 (2006).
15. S. Y. Chew, Y. Wen, Y. Dzenis and K. W. Leong, *Curr. Pharm. Design* **12**, 4751 (2006).
16. J. Lannutti, D. Reneker, T. Ma, D. Tomasko and D. Farson, *Mater. Sci. Eng. C* **27**, 504 (2007).
17. Q. P. Pham, U. Sharma and A. G. Mikos, *Tissue Eng.* **12**, 1197 (2006).
18. A. Greiner and J. H. Wendorff, *Angew. Chem. Int. Edn* **46**, 5670 (2007).
19. S. Ramakrishna, K. Fujihara, W.-E. Teo, T. Lim and Z. Ma, *An Introduction to Electrospinning and Nanofibers*. World Scientific Publishing, Singapore (2005).
20. S. Ramakrishna, K. Fujihara, W.-E. Teo, T. Yong, Z. Ma and R. Ramakrishna, *Mater. Today* **9**, 40 (2006).
21. W.-E. Teo and S. Ramakrishna, *Nanotechnology* **17**, R89 (2006).
22. M. M. Stevens and J. H. George, *Science* **310**, 1135 (2005).
23. L. Zhang and T. J. Webster, *Nanotoday* **4**, 66 (2009).
24. S. Krumm, *Acta Univ. Carol. Geol.* **38**, 253 (1994).
25. M. Kakudo and N. Kasai, *X-Ray Diffraction by Polymers*. Elsevier, New York, NY (1972).
26. V. Vichai and K. Kirtikara, *Nature Protocols* **1**, 1112 (2006).
27. V. V. Nikolaychik, M. M. Samet and P. I. Lelkes, *J. Biomater. Sci. Polymer Edn* **7**, 881 (1996).
28. P. Gupta, C. Elkins, T. E. Long and G. L. Wilkes, *Polymer* **46**, 4799 (2005).
29. S.-H. Tan, R. Inai, M. Kotaki and S. Ramakrishna, *Polymer* **46**, 6128 (2005).
30. S. L. Shenoy, W. D. Bates, H. L. Frisch and G. E. Wnek, *Polymer* **46**, 3372 (2005).

31. T. Jarusuwannapoom, W. Hongrojjanawiwat, S. Jitjaicham, L. Wannatong, M. Nithitanakul, C. Pattamaprom, P. Koombhongse, R. Rangkupan and P. Supaphol, *Eur. Polym. J.* **41**, 409 (2005).
32. D. R. Lide, *Handbook of Chemistry and Physics*. CRC Press, Boca Raton, FL (2007).
33. M. Li, M. J. Mondrinos, M. R. Gandhi, F. K. Ko, A. S. Weiss and P. I. Lelkes, *Biomaterials* **26**, 5999 (2005).
34. X. Zhong, K. Kim, D. Fang, S. Ran, B. S. Hsiao and B. Chu, *Polymer* **43**, 4403 (2002).
35. H. Fong and D. H. Reneker, *Polymer* **40**, 4585 (1999).
36. W. K. Son, J. H. Youk, T. S. Lee and W. H. Park, *Polymer* **45**, 2959 (2004).
37. K. H. Lee, H. Y. Kim, H. J. Bang, Y. H. Jung and S. G. Lee, *Polymer* **44**, 4029 (2003).
38. J. M. Deitzel, J. D. Kleinmeyer, J. K. Hirvonen and N. C. Beck Tan, *Polymer* **42**, 8163 (2001).
39. X. Zhong, S. Ran, D. Fang, B. S. Hsiao and B. Chu, *Polymer* **44**, 4959 (2003).
40. J. Hescheler, R. Meyer, S. Plant, D. Krautwurst, W. Rosenthal and G. Schultz, *Circulation Res.* **69**, 1476 (1991).